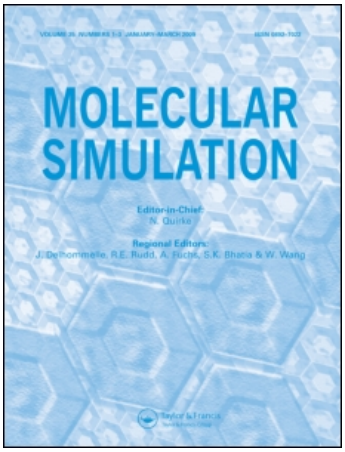

Molecular Simulation
Publication details, including instructions for authors and subscription information:
http://www.informaworld.com/smpp/title~content=t713644482

Heterogeneous or competitive self-assembly of surfactants and nanoparticles at liquid-liquid interfaces

Mingxiang Luo[a]; Yanmei Song[b]; Lenore L. Dai[b]
[a] Department of Chemical Engineering, Texas Tech University, Lubbock, TX, USA [b] Department of Chemical Engineering, Arizona State University, Tempe, AZ, USA

To cite this Article Luo, Mingxiang , Song, Yanmei and Dai, Lenore L.(2009) 'Heterogeneous or competitive self-assembly of surfactants and nanoparticles at liquid-liquid interfaces', Molecular Simulation, 35: 10, 773 — 784
To link to this Article: DOI: 10.1080/08927020902769851
URL: http://dx.doi.org/10.1080/08927020902769851

Molecular Simulation
Vol. 35, Nos. 10–11, September 2009, 773–784

Taylor & Francis
Taylor & Francis Group

Heterogeneous or competitive self-assembly of surfactants and nanoparticles at liquid–liquid interfaces

Mingxiang Luo[a1], Yanmei Song[b2] and Lenore L. Dai[b]*

[a]*Department of Chemical Engineering, Texas Tech University, Lubbock, TX 79409, USA;* [b]*Department of Chemical Engineering, Arizona State University, Tempe, AZ 85287, USA*

(*Received 19 December 2008; final version received 18 January 2009*)

We have performed molecular dynamics (MD) simulations to investigate self-assembly at water–trichloroethylene (TCE) interfaces with the emphasis on systems containing sodium dodecyl sulphate (SDS) surfactants and modified hydrocarbon nanoparticles (1.2 nm in diameter, non-charged and negatively charged, respectively). The surfactants and nanoparticles were first distributed randomly in the water phase. The MD simulations have clearly shown the progress of migration and final equilibrium of the SDS molecules at the water–TCE interfaces, with the non-charged nanoparticles either at or in the vicinity of the interfaces depending on surfactant concentrations. The non-charged nanoparticles co-equilibrate with the surfactants at the interfaces at low concentrations of surfactants; however, the surfactants, at high concentrations, competitively dominate the interfaces and deplete nanoparticles away from the interfaces. The interfacial properties, such as interfacial thickness and interfacial tension, are significantly influenced by the presence of the surfactant molecules, but not the non-charged nanoparticles. Interestingly, nanoparticle charge has a significant impact on interfacial assembly, structure and properties. The negatively charged nanoparticles co-equilibrate with the SDS surfactant molecules at the TCE–water interfaces, regardless of the surfactant concentration. Although the inclusion of the charged nanoparticles has a minor influence on the interfacial thickness, it significantly affects the distribution, ordering and effectiveness of the SDS surfactant molecules.

Keywords: interfacial self-assembly; molecular dynamics simulation; surfactants; nanoparticles

1. Introduction

Liquid–liquid interfaces are ubiquitous in daily lives. Interfacial self-assembly of nano-sized objects, such as surfactants and nanoparticles, serves as building blocks and is essential in various natural and industrial applications. For example, surfactant interfacial self-assembly is critical in numerous processes such as lubrication, detergency, biological transferring and polymer processing. On the other hand, self-assembled nanoparticles at a liquid–liquid interface serve as building blocks for bottom-up assembly of new functional materials with unique physical properties [1,2]. Furthermore, there is growing interest in solid-stabilised emulsions that use solid nanoparticles or microparticles as emulsion stabilisers. For these systems, the self-assembly of solid particles at liquid–liquid interfaces is essential [3–12]. However, it is important to note that many industrial processes are performed in the presence of both surfactants and nanoparticles. For example, the chemical flooding processes in tertiary (enhanced) oil recovery use surfactants, as high as 2–10% [13], but solid particles in the oil well, such as clays, scales and corrosion products can also self-assemble at the oil–water interfaces [14]; thus the interactions between surfactants and particles become important. As another example, in a multi-layer coating process, the competition of the surfactants (often for wetting purpose) and the nanoparticles (often for property enhancement purpose) at liquid–liquid interfaces is also not negligible. Recently, Binks and Rodrigues [8] have reported improved emulsion stability when using a mixture of oppositely charged silica nanoparticles and ionic surfactants as emulsion stabilisers. In spite of the importance, interfacial adsorption when a system contains both surfactants and colloidal particles has not been extensively studied. In particular, there is a limited understanding when nanoparticles are involved. One consensus is that the co-existence of surfactants and nanoparticles may influence each other on surface activities [5,15]. Very recently, there has been increasing attention and effort to understand the systems involving both surfactants and nanoparticles. Here, we use molecular dynamics (MD) simulations as a tool to study interfacial adsorption in the presence of both surfactants and nanoparticles (non-charged and negatively charged, respectively).

MD simulation is a powerful tool for obtaining molecularly detailed information and the underlying physics of various systems including liquid–liquid interfaces, with and without the presence of the nano-sized objects.

*Corresponding author. Email: lenore.dai@asu.edu

ISSN 0892-7022 print/ISSN 1029-0435 online

DOI: 10.1080/08927020902769851
http://www.informaworld.com

These simulations often provide molecular information that supplement experimental capabilities and have illuminated new insights. For example, MD simulations have been successfully performed on various water–organic solvent interfaces [16–22]. Moreira and Skaf [17] found a significant reduction of hydrogen bonds near the water–carbon tetrachloride interface and the dipole moments of water showed preference of aligning along the interface. The work by Zhang et al. [18] suggested that there were inner and outer layers near the water–octane interface and the water dipoles pointed in opposite directions at the different layers. Benjamin [21] investigated the self-diffusion of liquid molecules at water–dichloroethane interfaces and found that the diffusion of both water and dichloroethane molecules was faster parallel to the interface than when perpendicular to it. The MD simulations have also been extended to liquid–liquid interfaces containing surfactant molecules. Rivera et al. [23] simulated water–alkane systems containing methanol and reported the surfactant behaviour of methanol i.e. methanol molecules adsorbed preferably at the water–alkane interface and decreased the interfacial tension through molecular rearrangement. Schweighofer et al. [24] observed the inclination of sodium dodecyl sulphate (SDS) anionic surfactants at water–CCl_4 interfaces. The mixture of SDS with non-ionic surfactants was simulated by Dominguez [25] and the results showed that the interaction and charge distribution had significant effects on the location of surfactants. In contrast to the tremendous work of simulating liquid–liquid interfaces or interfaces containing surfactants, there are sparse simulations emphasising on interfacial nanoparticle assembly. To the best of our knowledge, we reported the first MD simulations investigating the self-assembly of nanoparticles at liquid–liquid interfaces [26]. The work has successfully simulated the *in situ* self-assembly of modified hydrocarbon nanoparticles at a water–trichloroethylene (TCE) interface [26]. In this report, we review and update some of our recent work of using MD simulations to investigate the heterogeneous or competitive self-assembly of surfactants and nanoparticles at the water–TCE interfaces. Specifically, we target the fundamental questions such as the influences of surfactant concentration on interfacial self-assembly and equilibrium structure, the effects of surfactants and nanoparticles on interfacial properties and finally, the impact of nanoparticle charge on interfacial assembly, structure and properties.

2. Methodology

2.1 Modelling

Water was modelled using the single point charge model [27,28]. The structures and topologies of SDS and TCE were generated by the small-molecule topology generator PRODRG [29]. The spherical modified hydrocarbon nanoparticle (mean diameter of 1.2 nm) was truncated from a diamond-like lattice made of carbon atoms that bonded in non-planar hexagonal structure and, to increase the simulation efficiency, saturated with united CH, CH_2 and CH_3 atoms [26,30]. For charged nanoparticles, the negatively charged site is modified on CH_3 united atom, and each particle has six negatively charged sites.

2.2 Composition of simulation systems

We have simulated four types of systems detailed as follows: system A was a 20 ns simulation of pure water and TCE; systems B were 50 ns simulations of water and TCE containing 5 and 10 nanoparticles, respectively; systems C were 50 ns simulations of water and TCE containing 5, 10, 20, 50 and 99 SDS molecules, respectively; systems D were 50 ns simulations of water and TCE containing 2, 5 and 10 nanoparticles and different number of SDS molecules, respectively. The self-assembly of SDS and negatively charged nanoparticles at water–TCE interfaces was also studied (D9–D13). In these systems, the net charge of the entire system was neutralised by adding positive sodium ions. For system D12 and D13, the simulation time was extended to 100 ns. Nanoparticles or SDS molecules were added into the water phase at the beginning of the simulations for systems B or C. The surfactants were added into the water phase after the nanoparticles' initial insertion at the beginning of the simulations for systems D. It is worthwhile noting that our approach is different from several other MD simulations [24,25,31] of liquid–liquid interfaces containing surfactants only, where the surfactants are initially pinned at the interfaces. In our simulations, the surfactants, as well as nanoparticles, were initially added into the water phase to empower the simulation to compute their dynamics in the two phases and final equilibrium positions. System A contains a total of 5913 atoms and the initial size of the simulation box is $3.3 \times 3.3 \times 7.8\,nm^3$. The initial size of the simulation box was $8.3 \times 8.3 \times 19.6\,nm^3$ for systems B and $10.4 \times 10.4 \times 20.6\,nm^3$ for systems C and D. The atom numbers are different in systems B, C and D due to the presence of different numbers of nanoparticles and surfactant molecules. All systems lead to an initial density of $1.0\,g\,cm^{-3}$ for water and $1.456\,g\,cm^{-3}$ for TCE. A summary of the computed systems is shown in Table 1.

2.3 Simulation details

The MD simulations were performed using the GROMACS 3.3.1 package [32–35]. The interaction parameters were computed using the GROMOS96 force field [36],

Table 1. Composition of the simulation systems.

System	Nanoparticle (particle)	SDS (molecule)	TCE (molecule)	Water (molecule)	Runs[a]
A1	0	0	288	1491	4
B1	5	0	4500	23,585	8
B2	10	0	4500	23,585	6
C1	0	5	5249	33,971	4
C2	0	10	5249	33,059	4
C3	0	20	5249	32,888	4
C4	0	50	5249	32,361	4
C5	0	99	5249	30,924	4
D1	2	5	5249	33,183	4
D2	5	10	5249	32,755	4
D3	5	20	5249	32,582	4
D4	5	50	5249	32,058	8
D5	5	99	5249	30,924	4
D6	10	20	5249	32,281	4
D7	10	50	5249	31,757	8
D8	10	99	5249	30,924	8
D9[b]	10	5	5249	32,485	4
D10	10	10	5249	32,402	4
D11	10	20	5249	32,221	4
D12	10	50	5249	31,697	4
D13	10	100	5249	30,875	4

[a] Number of parallel runs with different initial velocities from Maxwellian distribution. System A simulates 20 ns; D12 and D13 simulate 100 ns; and the other systems simulate 50 ns.
[b] D9–D13 contains six negatively charged nanoparticles, whereas B1–B2 and D1–D8 contain neutral charged nanoparticles.

with the intermolecular (non-bonded) potential represented as a sum of the Lennard-Jones force and pairwise Coulomb interaction. Long-range electrostatic forces were calculated using cut-off method for system D1–D8 and particle-mesh Ewald method for the other systems. The velocity Verlet algorithm was used for the numerical integrations [37], and the initial atomic velocities were generated with a Maxwellian distribution at the given absolute temperature [38,39]. After the construction of the simulation box, the energy was minimised using the steepest descent method with a cut-off radius of 10 Å for van der Waals and Coulomb forces. Simulations were performed in NPT (constant number of molecules, constant pressure and constant temperature) ensemble [40] using the Berendsen thermostat [41] with coupled temperature and pressure at 300 K and 1 bar. We used a 9 Å cut-off radius for van der Waals interactions and a 10 Å cut-off radius for long-range electrostatics (larger cut-off radius of 1.2 and 1.4 nm were also compared and led to negligible difference) [42]. Periodic boundary conditions were applied in all directions. The time step was 4 fs. The results were averaged from multiple parallel runs. The simulation details of systems A, B and C can be found in the previously published paper by our group [26,42]. After the simulation, the interfacial properties and structures were characterised using the GROMACS analysis tools and visual MD [43].

3. Results and discussions

3.1 Influences of surfactant concentration on interfacial self-assembly and equilibrium structure

The emphasis here is investigating the interfacial self-assembly of systems containing a mixture of surfactants and non-charged nanoparticles; for comparison, we have also included systems involving only surfactants or non-charged nanoparticles. Figure 1(a) shows the progress of cluster formation, migration and final equilibrium of 10 non-charged nanoparticles (B2) at the water–TCE interfaces, whereas Figure 1(b) computed the self-assembly of a system containing 99 surfactants (C5). It is noticeable that the surfactants equilibrate at the water–TCE interfaces at a much faster rate compared to that of the nanoparticles. Similar observations are made for the systems with different surfactant or non-charged nanoparticle concentrations.

Not surprisingly, the interfacial assembly becomes more complicated in the presence of both surfactants and nanoparticles. One intriguing observation is the effect of surfactant concentration on equilibrium structure. At low surfactant concentrations (D1-D4 and D6-D7), the surfactants and the non-charged nanoparticles can co-equilibrate at the same water–TCE interfaces, as demonstrated as an example in Figure 1(c). However, at the highest surfactant concentration when the systems contain 99 surfactants, the nanoparticles are depleted away from the interface at equilibrium (Figure 1(d)). This is likely due to the steric effect of surfactants although more detailed mechanism needs to be further explored. Recently, Vermant and co-workers [44,45] reported that adding SDS surfactant molecules to the polystyrene colloidal particles at oil–water interfaces pushed the particles into the oil phase due to a significant increase in contact angles. Although the colloidal particles (approximately 3 μm) in those experiments are several magnitudes larger compared to the nanoparticles here, it does raise the question whether or not a change of contact angle occurs and similar interpretation is applicable to the nanoparticle case.

In all simulated systems, the surfactants can attach to the nanoparticles and diffuse simultaneously with the nanoparticles in the water phase towards the interfaces. However, one unique characteristic is the 'detachment' of surfactants to the non-charged nanoparticles when reaching the water–TCE interface: surfactants will detach themselves from the nanoparticles and remain at the interfaces, whereas the nanoparticle clusters will diffuse further into the TCE phase. The nanoparticle clusters will finally equilibrate at the water–TCE interfaces except in the systems containing 99 surfactants, as discussed previously. Figure 2 is a snapshot of one sample run of system D8 at 21 ns when two nanoparticle clusters are in the vicinity of a water–TCE interface. The upper

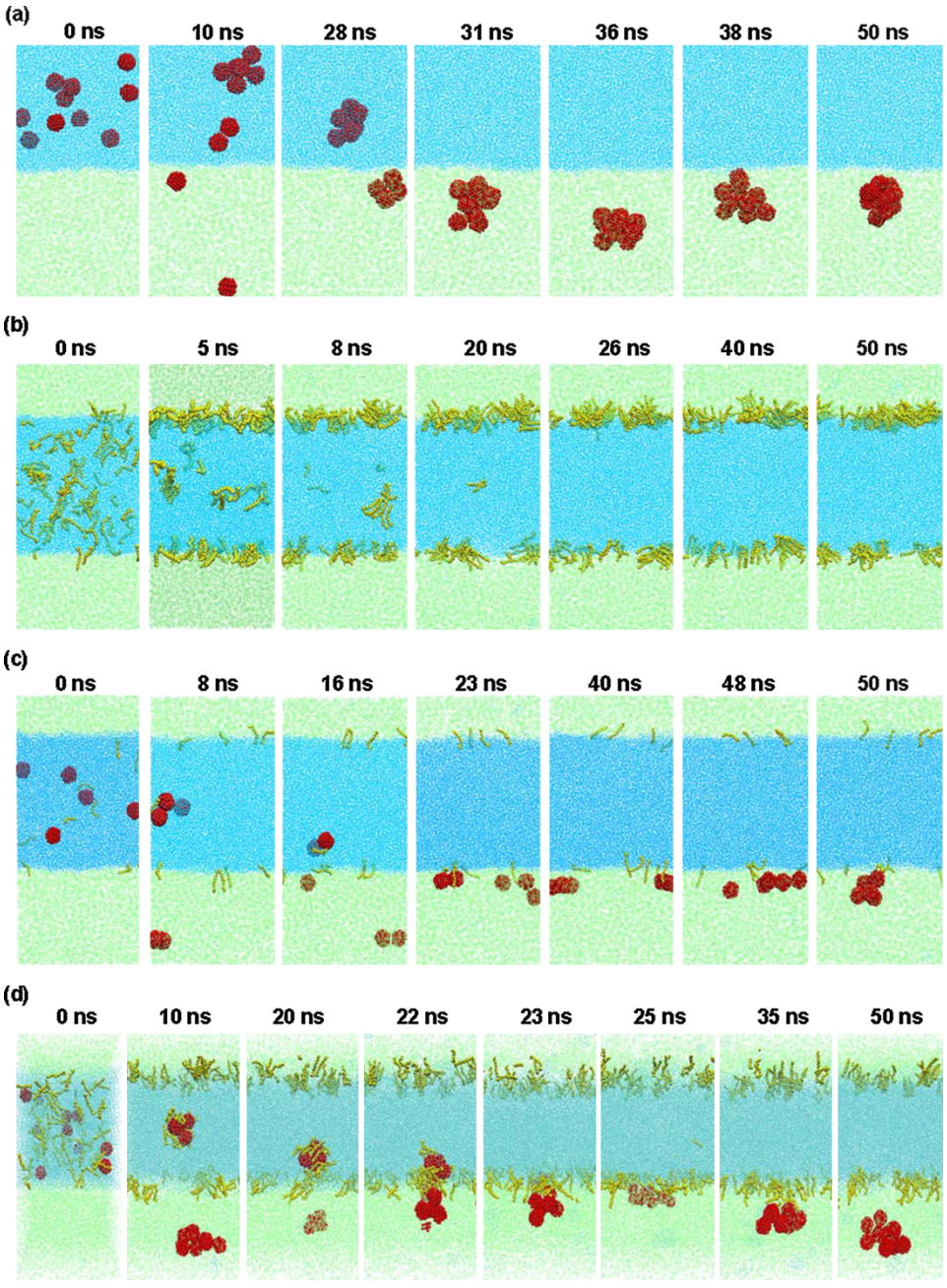

Figure 1. Sample snapshots of systems (a) B2, (b) C5, (c) D2 and (d) D8 at different simulation time intervals. The non-charged nanoparticles, SDS molecules, water phase and TCE phase are represented in red, yellow, blue and lime, respectively.

nanoparticle cluster surrounded by surfactants is approaching the interface and the lower nanoparticle cluster is diffusing away from the interface.

3.2 Effects of surfactants and nanoparticles on interfacial properties

One intuitive question to ask is the influences of surfactants and nanoparticles on interfacial properties such as interfacial thickness and interfacial tensions. Figure 3(a) presents the mass density profile of a pure water–TCE system (system A) and Figure 3(b)–(d) are those of systems containing nanoparticles (system B2), or surfactants (system C5), or both (systems D2 and D8). Interfacial thickness, defined as the distance over which the TCE density drops from 90 to 10% of the bulk density, is plotted as a function of number of SDS surfactants in Figure 4. It illustrates a monotonic increase of the interfacial thickness with increasing number of SDS surfactants. Luo et al. [26] have shown that the water–TCE interface thickness is increased by

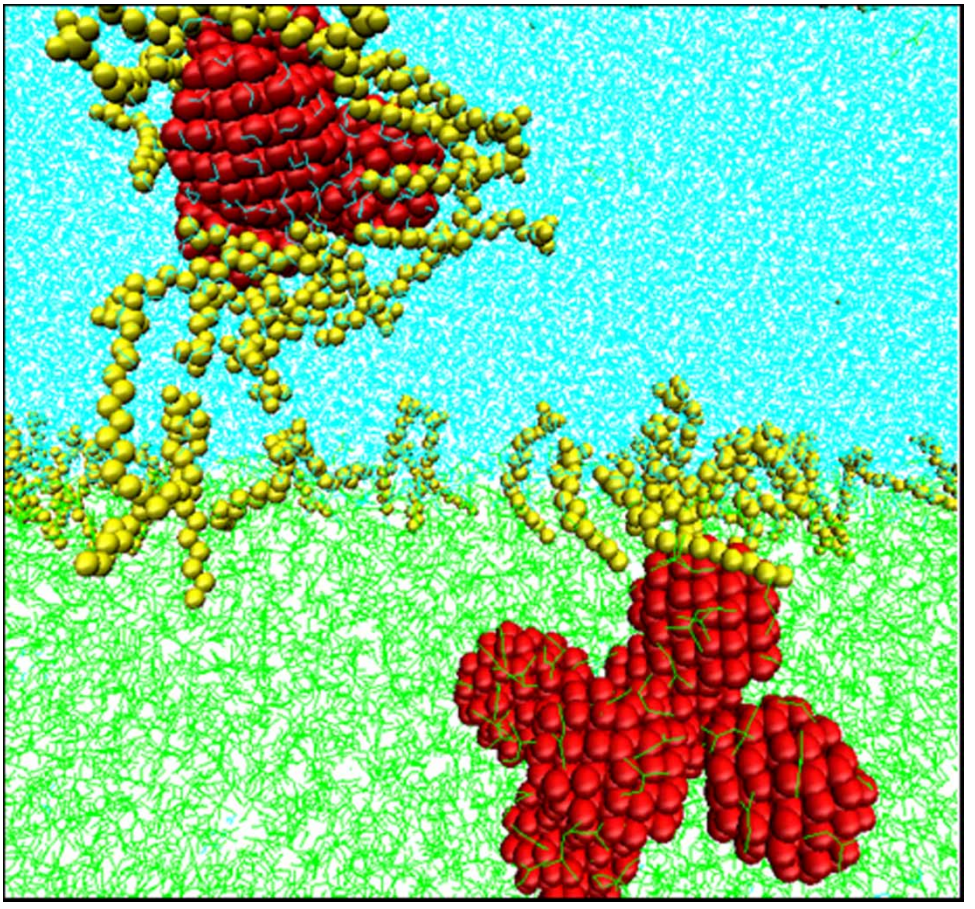

Figure 2. Snapshot of one sample run of system D8 at 21 ns. Four non-charged nanoparticles form a cluster in water and six non-charged nanoparticles form a cluster in TCE. The non-charged nanoparticles, SDS molecules, water phase and TCE phase are represented in red, yellow, blue and lime, respectively.

approximately 40% with the presence of nanoparticle clusters either near or in contact with the interface, but is independent of the number of nanoparticles present. Figure 4 illustrates that the nanoparticles may also affect the interfacial thickness but their influences is significantly less compared to that of the surfactants. The strong effect of SDS surfactants on interfacial thickness is also observed by the MD simulation by Schweighofer et al. [24] in which they studied the SDS at water–CCl_4 interfaces, although the latter involves surfactants only. Recently, Li et al. [46] have reported that the dodecane–water interfacial thickness increases with increasing the concentrations of linear alkanesulphonate and alkybenzenesulfonates using a dissipative particle dynamics simulation. According to the theoretical work by Telo da Gama et al. [47], the increased interfacial thickness is due to the accommodation of the presence of concentrated surfactants at the interface.

Another important physical property is interfacial tension (γ), which is calculated using

$$\gamma = \frac{1}{2}\left\langle L_z\left(p_{zz} - \frac{p_{xx}+p_{yy}}{2}\right)\right\rangle, \qquad (1)$$

where $p_{\alpha\alpha}$ ($\alpha = x$, y, or z) is the $\alpha\alpha$ element of the pressure tensor and L_z is the linear dimension of the simulation cell in the z direction perpendicular to the interfaces [18,23,39]. Figure 5 shows the normalised water–TCE interfacial tension as a function of the number of SDS molecules in systems C and D. The interfacial tension is normalised by dividing the interfacial tension of each system with the interfacial tension of pure water–TCE. The pure water–TCE interfacial tension, simulated from system A, is 41.5 mN/m, which is reasonably close to the experimental value of 38.9 mN/m measured in our laboratory using a Krüss K100 tensiometer. Figure 5 shows that the increasing number of SDS molecules results in a significant reduction of interfacial tension. The reduction slows down at higher SDS concentrations. It is noticeable that here nanoparticles have a minor influence on interfacial tension, which is consistent with the observation on systems B. Surfactants such as SDS molecules are well-known for effective reduction of interfacial tensions. Similar reduction has been observed in the MD simulations of water–vapour and water–CCl_4 interfaces containing surfactants [48]. The reduction of surfactants on interfacial tension has also been

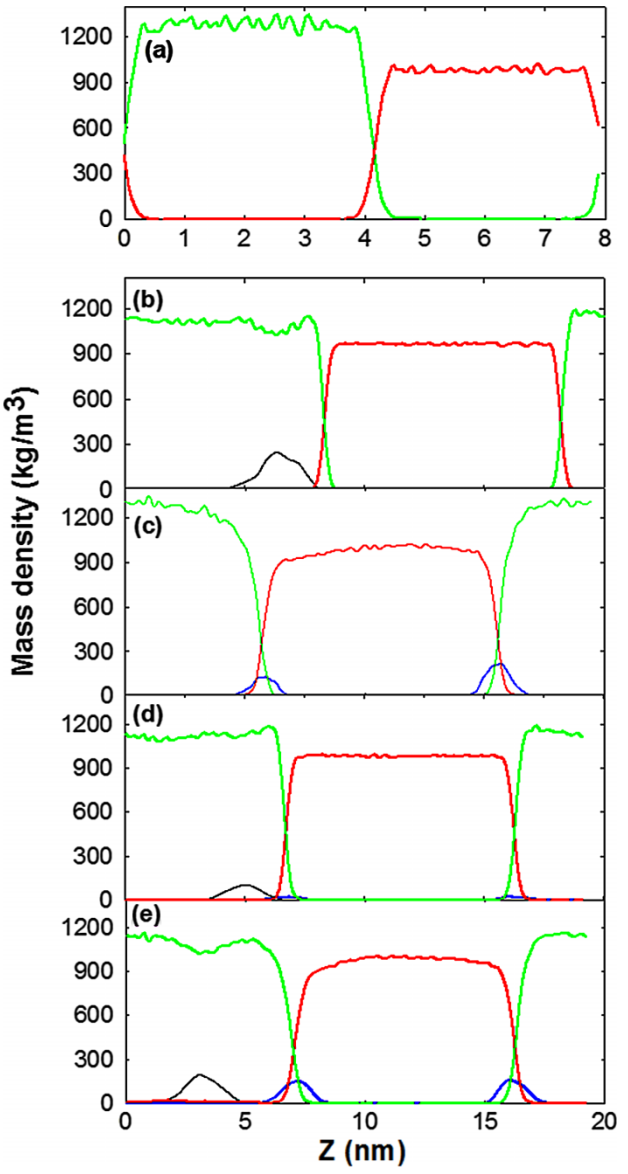

Figure 3. Mass density profiles for systems (a) A, (b) B2, (c) C5, (d) D2 and (e) D8 obtained by dividing the simulation cell into 100 slabs parallel to the water–TCE interface. Densities were averaged over the last 1 ns. The nanoparticles, SDS, water and TCE molecules are represented in black, blue, red and green, respectively.

studied extensively from experimental and practical aspects. One prevailing mechanism is proposed by Langmuir in which the reduction of surface tension is equivalent to the pressure of the two-dimensional surfactant film [49]. The theoretical work by Telo da Gama et al. [47] used a generalised van der Waals model and suggested that the reduction in surface tension is proportional to adsorbed surfactants only at low concentrations but the correlation fails at high interfacial surfactant concentrations. In contrast, there is sparse work on the effect of nanoparticles on interfacial tension. Recently, Ravera et al. [50] have

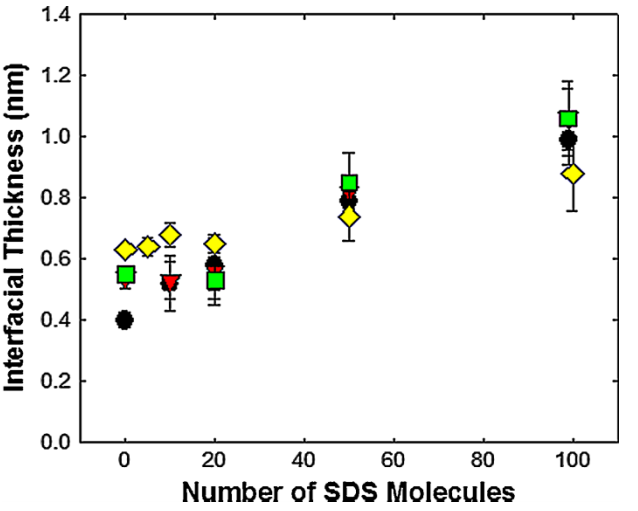

Figure 4. Interfacial thickness as a function of the number of SDS molecules. The circles, triangles, squares and diamonds represent interfacial thickness of the systems without nanoparticles and with 5, 10 non-charged and 10 negatively charged nanoparticles, respectively.

reported the experimental work on the influence of colloidal silica nanoparticles on interfacial tensions of water–air and water–hexane interfaces containing hexadecyltrimethylammonium bromide (CTAB) surfactant using a drop shape tensiometer. Their work showed that the presence of 1 wt % nanoparticles significantly reduced the effectiveness of CTAB due to the adsorption of surfactants onto nanoparticles and led to a reduction of surfactant concentration at the interface. Here we use nanoparticles (1.2 nm in diameter) that are more than a magnitude smaller compared to those in the experimental work. In addition, the simulation has clearly shown that although the SDS

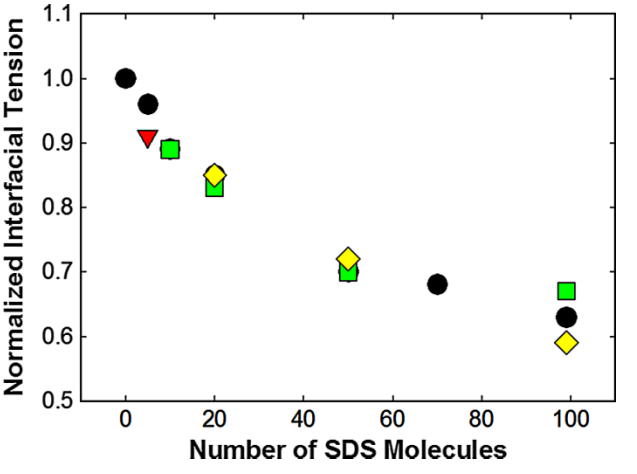

Figure 5. Normalised water–TCE interfacial tensions as a function of the number of surfactant molecules. The circles, triangles, squares and diamonds represent interfacial tensions of the systems without the nanoparticles and with 2, 5 and 10 nanoparticles, respectively.

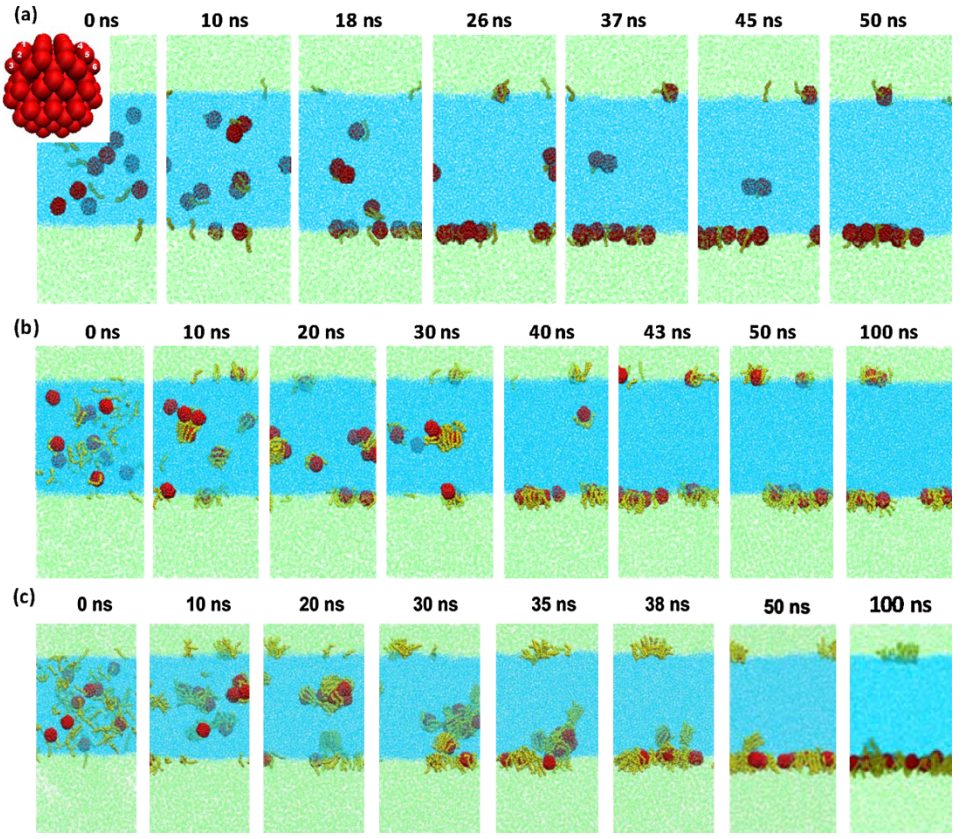

Figure 6. Sample snapshots of systems (a) D10, (b) D12 and (c) D13 at different simulation time intervals. The negatively charged nanoparticles, SDS molecules, water phase and TCE phase are represented in red spheres, in yellow, in blue and in lime, respectively. The inset in (a) shows the morphology and charge-sites (labelled 1–6) of the nanoparticles.

surfactants attach to the nanoparticles in the water phase, they detach themselves when reaching the interface and remain final equilibration at the interfaces. We hypothesise that the minor effect of nanoparticle clusters on interfacial tension here may also be explained by their small contact area with the interface (only one or two particles within the clusters are 'truly' in contact with the interface), thus the effect on interfacial pressure is less significant.

3.3 Effects of nanoparticle charges on interfacial assembly, structure and properties

We started our study using the non-charged nanoparticles but have realised that charged nanoparticles are often more prevalent and technologically important due to their better dispersibility and stability. In this section, we will reveal some interesting characteristics of systems involving surfactants and charged nanoparticles. The nanoparticles here are negatively charged and have six negatively charged sites, as illustrated in the inset of Figure 6(a), and make significant impacts on interfacial assembly and properties. First, in contrast to non-charged nanoparticles being depleted away from the TCE–water interfaces, the charged nanoparticles remain at the interface and form a monolayer, even at the highest surfactant concentration (100 surfactants). Figure 6(a)–(c) shows snapshots of the *in situ* self-assembly of surfactants and charged nanoparticles in systems D10, D12 and D13, respectively. In all systems, the surfactants and nanoparticles heterogeneously co-equilibrate at the water–TCE interfaces. One preliminary hypothesis is that the affinity between the charged sites and water may play an important role for the charged nanoparticles to be 'confined' at the interfaces. Recently, experiments have shown that the interfacial assembly of nanoparticles alone can be tuned by the surface charge density [51,52] although the complexity due to the involvement of the surfactants here makes it hard to compare.

It is worthwhile to note that the charge also affects the morphology of the SDS molecules when they are in contact with the nanoparticles. For the non-charged nanoparticles, the hydrophobic tails of the SDS molecules orient closer to the nanoparticle surfaces with the hydrophilic heads pointing outwards, as shown in Figure 7(a). This is mainly due to the hydrophobic nature of the nanoparticles, the hydrophilic nature of the surrounding water phase and the amphiphilic nature of the SDS molecules. Interestingly, the morphology changes

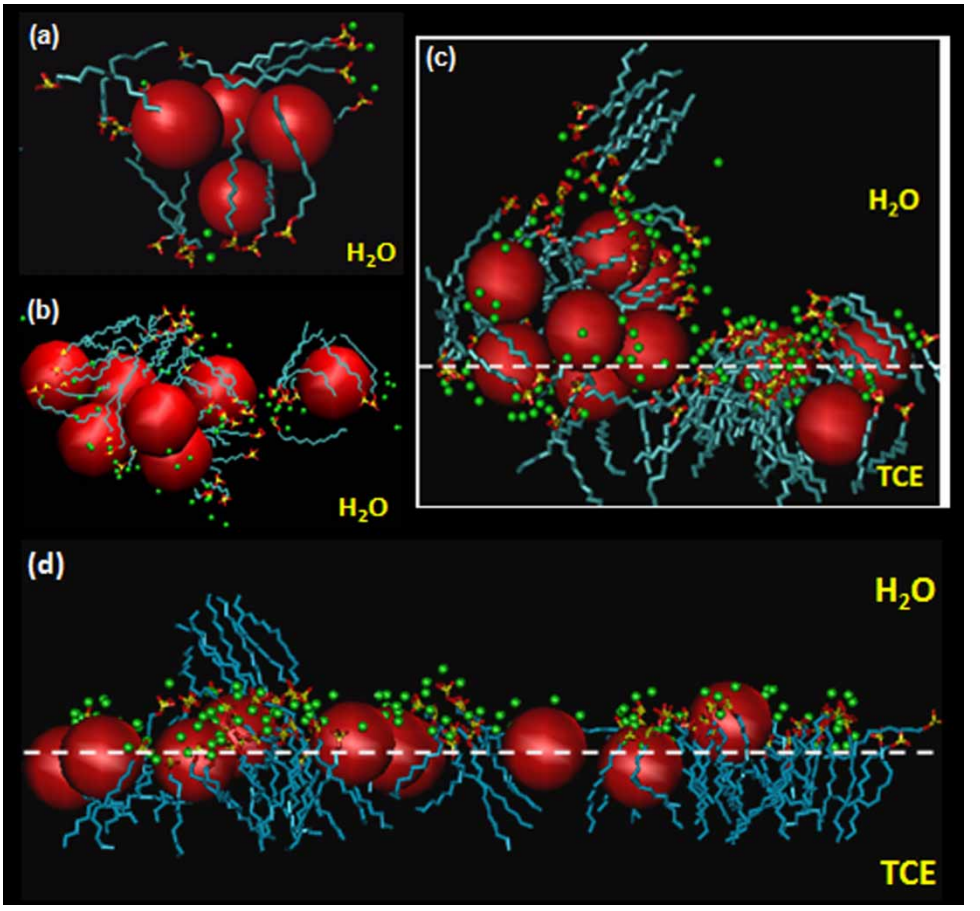

Figure 7. Sample snapshots showing the morphology of surfactant molecules in contact with nanoparticles. (a) System D8 at 10 ns (in water); (b) D13 at 20 ns (in water); (c) D13 at 35 ns (at a water–TCE interface); (d) D13 at 100 ns (at a water–TCE interface). The nanoparticles are represented as simplified red balls. The hydrophobic chains of SDS molecules are represented in blue chains and the hydrophilic head groups of SDS molecules are represented in red and yellow. Sodium ions are in green.

when the negatively charged nanoparticles are present. Figure 7(b) is a snapshot showing the SDS surfactant molecules and charged nanoparticle cluster of system D13 in the water phase at 20 ns. It appears that most of the hydrophobic tails of the SDS molecules orient closer to the nanoparticle surfaces compared to the non-charged ones and surprisingly, some of the hydrophilic heads are also pointing inwards and the surfactant molecules lay adjacent to the nanoparticles. Many sodium ions can be observed close to the hydrophilic heads of the surfactants or nearby the nanoparticle surfaces. A more detailed investigation shows that the hydrophilic heads are closer to the negatively charged sites of the nanoparticles. The detailed mechanism is not fully understood, although a double layer effect would be a reasonable initial guess, which is the six negatively charged sites on the nanoparticles attract some positively charged sodium ions, and these sodium ions further attract a number of negatively charged surfactant hydrophilic heads. Such hypothesis seems to be magnified when the surfactant-nanoparticle clusters are approaching the interface (Figure 7(c)) and finally equilibrate at the water–TCE interfaces (Figure 7(d)). However, a more thorough investigation is needed.

Now let us turn into the influences of nanoparticle charge on interfacial properties. Figure 4 includes the interfacial thickness as a function of SDS concentration for systems involving charged nanoparticles. It appears that the charged nanoparticles have minor influences on the interfacial thickness. Figure 4 only includes the systems involving 10 charged nanoparticles and further analysis shows that the interfacial thickness slightly increases with increasing the concentrations of charged nanoparticles at the interfaces. However, the effect is minor comparing that of the surfactant concentration. In contrast, the inclusion of 10 negatively charged nanoparticles makes a tremendous impact on the interfacial tensions. Figure 5 shows that the normalised interfacial tension decreases significantly by increasing the number of surfactant SDS molecules, with and without the presence of non-charged nanoparticles. Surprisingly, the interfacial tension remains relatively constant, 41.0–43.7 mN/m with the presence of 10 negatively charged nanoparticles, when the number of

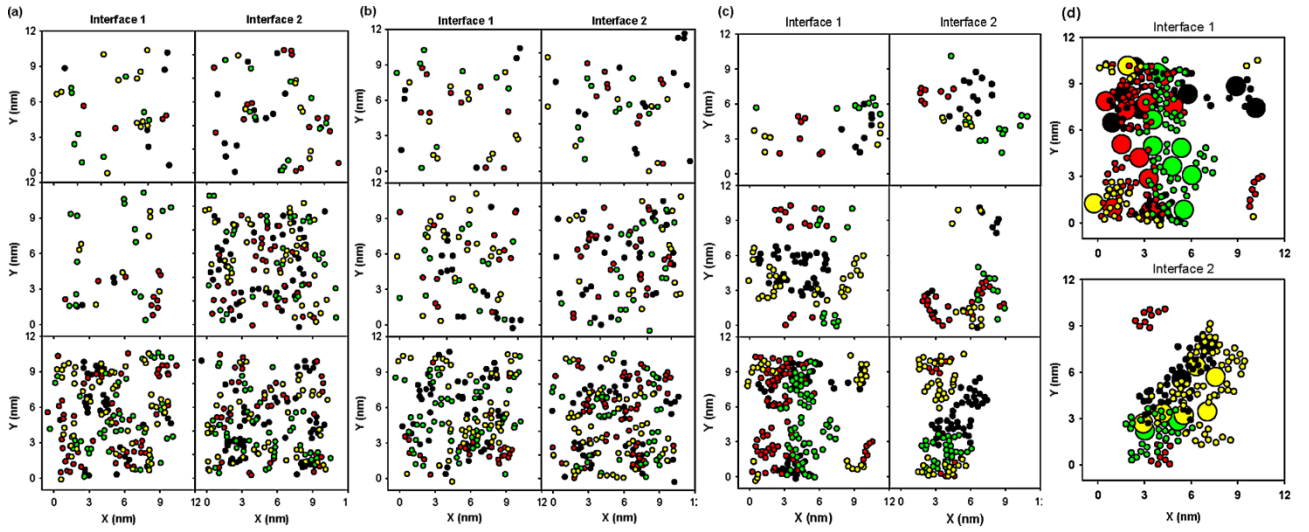

Figure 8. Lateral distribution of SDS molecules at water–TCE interfaces at equilibrium. Each point represents the centre of mass and the size of the circles corresponds to the cross area of SDS molecules. Parallel runs are represented in different colours. Panels from top to bottom are systems containing 20, 50 and 99 surfactants, respectively. (a) Systems without nanoparticles, C3, C4 and C5; (b) systems with non-charged nanoparticles, D6, D7 and D8; (c) systems with charged nanoparticles, D11, D12 and D13; (d) a sample illustration of the aggregation of the surfactant molecules with the charged nanoparticles in system D13; larger and smaller circles represent the actual size of nanoparticles and SDS molecules.

SDS molecules changes from 0 to 100. In order to understand the influence of charged nanoparticles on the performance of SDS molecules, we take the advantages that MD simulations provide detailed structural information at the molecular level. First, we compare the lateral distribution of the SDS molecules at the water–TCE interfaces under different scenarios. Figure 8(a) illustrates the lateral distribution of the SDS molecules (centre mass) at each interface, including all parallel runs of systems C3 (top panels), C4 (middle panels) and C5 (bottom panels). The parallel runs for each system are represented in different colours. The size of the circles shows the cross area of the SDS molecules. Although increasing the surfactant concentration causes an increasing degree of aggregation, the surfactant molecules distribute relatively even across the entire interfaces. The presence of non-charged nanoparticles, either at or in the vicinity of the interface, does not significantly alter the aggregation of surfactants, as qualitatively shown in Figure 8(b). However, Figure 8(c),(d) suggest that the charged nanoparticles attract the surfactants to aggregate surround the nanoparticles and unevenly distribute at the water–TCE interfaces. The latter may offer a preliminary explanation on why the presence of charged nanoparticles disfunctionalises the SDS surfactants' ability to lower the interface tensions.

Another noticeable effect of the nanoparticle charge is on the ordering of SDS surfactant molecules. Our simulation has shown that the anionic head groups (SO_4^-) of the SDS molecules immersed in the water phase with the tail groups (hydrocarbon chains) stretch across the interface into the TCE phase, when the systems involve surfactants or surfactants/non-charged nanoparticles. In other words, the surfactants span across the water–TCE interface microscopically. This is due to the hydrophilic and hydrophobic nature of their head and tail groups, respectively. The ordering of the surfactants is often characterised by a deuterium order parameter (S_{CD}), which is 'the average inclination of the C–D bond with respect to surface normal' [31]. The deuterium order parameter originates from the nuclear magnetic resonance experiments on lipid bilayers in which the hydrogen atoms are replaced by deuterium atoms [53]. The deuterium order parameter can be calculated as following [31]:

$$S_{CD} = \frac{1}{2}\langle 3\cos^2\theta_{CD} - 1\rangle, \qquad (2)$$

where θ_{CD} is the angle between the interfacial normal and the molecular axis of the surfactant. The two extremes of the deuterium order parameters are 1 and $-1/2$, corresponding to a perfect order along the interface normal and a perfect order along the interface. The value equals zero if the surfactants pack isotropically at the interface.

Figure 9 plots the influence of surfactant and particle concentration (non-charged and charged, respectively) on the deuterium order parameter of the SDS tail chain. As shown in Figure 9(a), the order parameter decreases for the carbon atoms further away from the head group, which

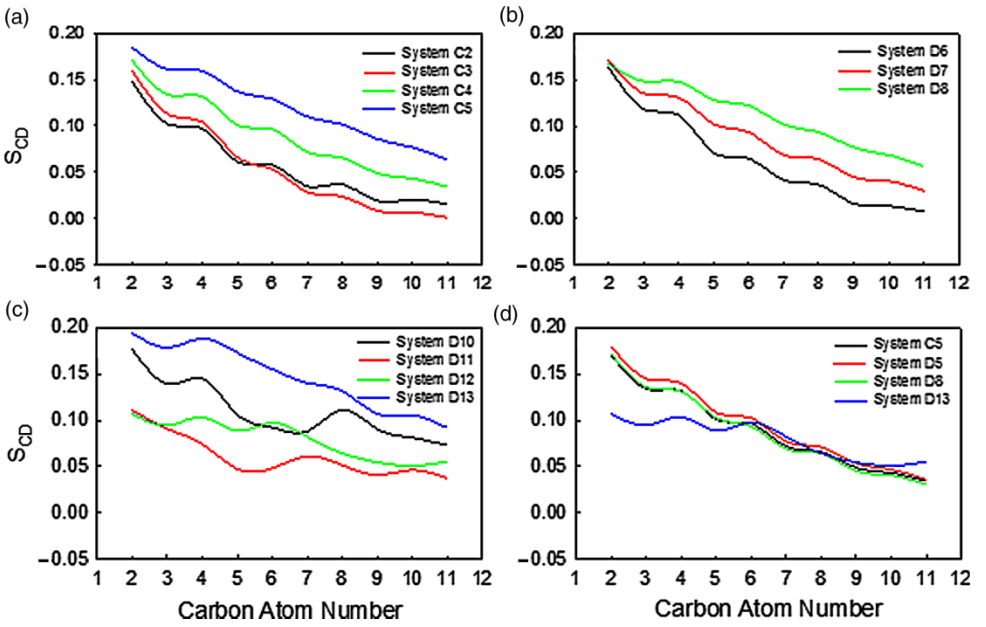

Figure 9. The deuterium order parameter (S_{CD}) as a function of carbon atom number starting '2' for the carbon atom adjacent to the head group. (a) Influence of SDS concentration; (b) influence of SDS concentration with the presence of non-charged nanoparticles; (c) influence of SDS concentration with the presence of negatively charged nanoparticles; (d) influence of nanoparticle concentration.

indicates more flexibility toward the tail end. However, S_{CD} increases with increasing SDS concentration, thus suggesting that SDS carbon chains become more ordered along the interfacial normal at higher SDS concentrations. The increased ordering as a function of increasing surfactant concentration has been observed in other simulations [25,46,54] and experiments [55,56]. For systems C and D containing 99 surfactants, the average interfacial area is 210 Å^2/molecule, which is significantly higher that the saturation value of 59 Å^2/molecule for a monolayer of SDS at water–CCl_4 interfaces [25]. In contrast to the result that the non-charged nanoparticles remain the same trend as that of surfactant alone (Figure 9(b)), the charged nanoparticles cause the SDS carbon chains more disordered, as shown in Figure 9(c). The carbon atoms near the head group are also noticeably bended along the interface plane (not shown). These may be explained by the fact that charged nanoparticles co-exist with SDS surfactants at the water–TCE interfaces and occupy a significant interfacial area, therefore the hydrophobic interaction between charged nanoparticles and SDS carbon chains and the electrostatic interactions between sodium ions, charged particles and SDS head groups alter the surfactant molecules to a relatively preferable orientation. Finally, Figure 9(d) shows that the order parameter is less influenced by the non-charged nanoparticles, which can be hypothesised by the fact that these nanoparticle clusters only have one or two particles in contact with the interface. The charged nanoparticles lower the ordering of the first several carbon atoms due to their strong interactions with the hydrophilic heads of the surfactant molecules.

4. Conclusion

MD simulations have been performed to investigate the self-assembly at water–TCE interfaces with the focuses on systems containing SDS surfactant molecules and modified hydrocarbon nanoparticles (non-charged and charged, respectively). To the best of our knowledge, the work provides the first MD simulation of the *in situ* interfacial self-assembly when a system contains both surfactants and nanoparticles. The MD simulations have clearly shown the progress of migration and final equilibrium of the SDS molecules at the water–TCE interfaces with the non-charged nanoparticles either at or in the vicinity of the interfaces, depending on surfactant concentrations. The non-charged nanoparticles co-equilibrate with the surfactants at the interfaces at low concentrations of surfactants whereas they are depleted away from the interfaces when the surfactant concentration is high. The interfacial properties, such as interfacial thickness and interfacial tension, are significantly influenced by the presence of the surfactants, but not the nanoparticles. Interestingly, nanoparticle charge has a significant impact on interfacial assembly, structure and properties. The negatively charged nanoparticles co-equilibrate with the SDS surfactant molecules at the TCE–water interfaces, regardless of the surfactant

concentration. Although the inclusion of the charged nanoparticles has a minor influence on the interfacial thickness, it significantly affects the distribution, ordering and effectiveness of the SDS surfactant molecules.

Acknowledgements

We thank the Texas Tech High Performance Computing Center (HPCC) and the Arizona State University Fulton High Performance Computing for computational resources. We are also grateful to the financial support from the National Science Foundation (CBET-0644850) and the American Chemical Society PRF fund.

Notes

1. Email: mx.luo@ttu.edu
2. Email: ysong30@asu.edu

References

[1] Y. Lin, H. Skaff, T. Emrick, A.D. Dinsmore, and T.P. Russell, *Nanoparticle assembly and transport at liquid–liquid interfaces*, Science 299 (2003), pp. 226–229.
[2] Y. Lin, H. Skaff, A. Böker, A.D. Dinsmore, T. Emrick, and T.P. Russell, *Ultrathin cross-linked nanoparticle membranes*, J. Am. Chem. Soc. 125 (2003), pp. 12690–12691.
[3] E.J. Stancik and G.G. Fuller, *Connect the drops: using solids as adhesives for liquids*, Langmuir 20 (2004), pp. 4805–4808.
[4] S. Melle, M. Lask, and G.G. Fuller, *Pickering emulsions with controllable stability*, Langmuir 21 (2005), pp. 2158–2162.
[5] H. Xu, S. Melle, K. Golemanov, and G.G. Fuller, *Shape and buckling transitions in solid-stabilized drops*, Langmuir 21 (2005), pp. 10016–10020.
[6] A.D. Dinsmore, M.F. Hsu, M.G. Nikolaides, M. Marquez, A.R. Bausch, and D.A. Weitz, *Colloidosomes: selectively permeable capsules composed of colloidal particles*, Science 298 (2002), pp. 1006–1009.
[7] T.S. Horozov, R. Aveyard, J.H. Clint, and B. Neumann, *Particle zips: vertical emulsion films with particle monolayers at their surfaces*, Langmuir 21 (2005), pp. 2330–2341.
[8] B.P. Binks and J.A. Rodrigues, *Enhanced stabilization of emulsions due to surfactant-induced nanoparticle*, Langmuir 23 (2007), pp. 7436–7439.
[9] J.L. Dickson, B.P. Binks, and K.P. Johnston, *Stabilization of carbon dioxide-in-water emulsions with silica nanoparticles*, Langmuir 20 (2004), pp. 7976–7983.
[10] N. Saleh, T. Sarbu, K. Sirk, G.V. Lowry, K. Matyjaszewski, and R.D. Tilton, *Oil-in-water emulsions stabilized by highly charged polyelectrolyte-grafted silica nanoparticles*, Langmuir 21 (2005), pp. 9873–9878.
[11] S. Tarimala and L.L. Dai, *Structure of microparticles in solid-stabilized emulsions*, Langmuir 20 (2004), pp. 3492–3494.
[12] L.L. Dai, R. Sharma, and C.Y. Wu, *Self-assembled structure of nanoparticles at a liquid–liquid interface*, Langmuir 21 (2005), pp. 2641–2643.
[13] V. Pillai, J.R. Kanicky, and D.O. Shah, *Handbook of Microemulsion Science and Technology*, Marcel Dekker, New York, 1999.
[14] S. Kokal, *Crude-oil emulsions: a state-of-the-art review*, SPE Prod. Facil. 20 (2005), pp. 5–13.
[15] H. Ma, M.X. Luo, and L.L. Dai, *Influences of surfactant and nanoparticle assembly on effective interfacial tensions*, Phys. Chem. Chem. Phys. 10 (2008), pp. 2207–2213.
[16] S. Senapati and M.L. Berkowitz, *Computer simulation study of the interface width of the liquid/liquid interface*, Phys. Rev. Lett. 8717 (2001), 176101.
[17] N.H. Moreira and M.S. Skaf, *Structural characterization of the H_2O/CCl_4 liquid interface using molecular dynamics simulations*, Prog. Colloid Polym. Sci. 128 (2004), pp. 81–85.
[18] Y.H. Zhang, S.E. Feller, B.R. Brooks, and R.W. Pastor, *Computer-simulation of liquid/liqid interfaces. 1. Theory and application to octane/water*, J. Chem. Phys. 103 (1995), pp. 10252–10266.
[19] A.R. Vanbuuren, S.J. Marrink, and H.J.C. Berendsen, *A molecuar-dynamics study of the decane–water interface*, J. Phys. Chem. 97 (1993), pp. 9206–9212.
[20] P.A. Fernandes, M.N.D.S. Cordeiro, and J.A.N.F. Gomes, *Molecular dynamics simulation of the water/1,2-dichloroethane interface*, J. Mol. Struct. Theochem. 463 (1999), pp. 151–156.
[21] I. Benjamin, *Theoretical-study of the water/1,2-dichloroethane interface—Structure, dynamics, and conformational equilibria at the liquid/liquid interface*, J. Chem. Phys. 97 (1992), pp. 1432–1445.
[22] L.X. Dang, *Intermolecular interactions of liquid dichloromethane and equilibrium properties of liquid–vapor and liquid–liquid interfaces: a molecular dynamics study*, J. Chem. Phys. 110 (1999), pp. 10113–10122.
[23] J.L. Rivera, C. McCabe, and P.T. Cummings, *Molecular simulations of liquid–liquid interfacial properties: water–*n*-alkane and water–methanol–*n*-alkane systems*, Phys. Rev. E 67 (2003), 011603.
[24] K.J. Schweighofer, U. Essmann, and M. Berkowitz, *Simulation of sodium dodecyl sulfate at the water–vapor and water–carbon tetrachloride interfaces at low surface coverage*, J. Phys. Chem. B 101 (1997), pp. 3793–3799.
[25] H. Dominguez, *Computer simulations of surfactant mixtures at the liquid/liquid interface*, J. Phys. Chem. B 106 (2002), pp. 5915–5924.
[26] M.X. Luo, O.A. Mazyar, Q. Zhu, M.W. Vaughn, W.L. Hase, and L.L. Dai, *Molecular dynamics simulation of nanoparticle self-assembly at a liquid–liquid interface*, Langmuir 22 (2006), pp. 6385–6390.
[27] H.J.C. Berendsen, J.P.M. Postma, W.F. Gunsteren, and J. Hermans, *Intermolecular Forces*, Reidel, Dordrecht, 1981.
[28] H.J.C. Berendsen, J.R. Grigera, and T.P. Straatsma, *The missing term in effective pair potentials*, J. Phys. Chem. 91 (1987), pp. 6269–6271.
[29] A.W. Schuttelkopf and D.M.F. van Aalten, *PRODRG: a tool for high-throughput crystallography of protein–ligand complexes*, Acta Crystallogr., Sect. D: Biol. Crystallogr. 60 (2004), pp. 1355–1363.
[30] O.A. Mazyar and W.L. Hase, *Dynamics and kinetics of heat transfer at the interface of model diamond {1 1 1} nanosurfaces*, J. Phys. Chem. A 110 (2006), pp. 526–536.
[31] K.J. Schweighofer, U. Essmann, and M. Berkowitz, *Structure and dynamics of water in the presence of charged surfactant monolayers at the water–CCl_4 interface: a molecular dynamics study*, J. Phys. Chem. B 101 (1997), pp. 10775–10780.
[32] H.J.C. Berendsen, D. Vanderspoel, and R. Vandrunen, *GROMACS–A message-passing parallel molecular dynamics implementation*, Comput. Phys. Commun. 91 (1995), pp. 43–56.
[33] E. Lindahl, B. Hess, and D. Van der Spoel, *GROMACS 3.0: A package for molecular simulation and trajectory analysis*, J. Mol. Model. 7 (2001), pp. 306–317.
[34] D. Van der Spoel, E. Lindahl, B. Hess, G. Groenhof, A.E. Mark, and H.J.C. Berendsen, *GROMACS: fast, flexible, and free*, J. Comput. Chem. 26 (2005), pp. 1701–1718.
[35] Q. Zhu and M.W. Vaughn, *Surface tension effect on transmembrane channel stability in a model membrane*, J. Phys. Chem. B 109 (2005), pp. 19474–19483.
[36] W.F. van Gunsteren, S.R Billeter, A.A. Eising, P.H. Hüenberger, P. Krüger, A.E. Mark, W.R.P. Scott, and I.G. Tironi, *Biomolecular Simulation: The GROMOS 96 Manual and User Guide*, Vdf Hochschulverlag, Zurich, 1996.
[37] C.S. William, C.A. Hans, H.B. Peter, and K.R.A. Wilson, *Computer-simulation method for the calculation of equilibrium-constants for the formation of formation of physical clusters of molecules-application to small water clusters*, J. Chem. Phys. 76 (1982), pp. 637–649.
[38] E.H. Kennard, *Kinetic Theory of Gases*, McGraw-Hill, New York, 1963.
[39] K. Huang, *Statistical Mechanics*, Wiley, New York, 1963.

[40] H.C. Andersen, *Molecular-dynamics simulations at constant pressure and/or temperature*, J. Chem. Phys. 72 (1980), pp. 2384–2393.
[41] H.J.C. Berendsen, J.P.M. Postma, W.F. van Gunsteren, A. DiNola, and J.R. Haak, *Molecular-dynamics with coupling to an external bath*, J. Chem. Phys. 81 (1984), pp. 3684–3690.
[42] M.X. Luo and L.L. Dai, *Molecular dynamics simulations of surfactant and nanoparticle self-assembly at liquid–liquid interfaces*, J. Phys.: Condens. Matter 19 (2007), 375109.
[43] W. Humphrey, A. Dalke, and K. Schulten, *VMD: visual molecular dynamics*, J. Mol. Graphics 14 (1996), pp. 33–38.
[44] B.J. Park, J.P. Pantina, E.M. Furst, M. Oettel, S. Reynaert, and J. Vermant, *Direct measurements of the effects of salt and surfactant on interaction forces between colloidal particles at water–oil interfaces*, Langmuir 24 (2008), pp. 1686–1694.
[45] S. Reynaert, P. Moldenaers, and J. Vermant, *Control over colloidal aggregation in monolayers of latex particles at the oil–water interface*, Langmuir 22 (2006), pp. 4936–4945.
[46] Y. Li, X.J. He, X.L. Cao, Y.H. Shao, Z.Q. Li, and F.L. Dong, *Mesoscopic simulation study on the efficiency of surfactants adsorbed at the liquid/liquid interface*, Mol. Simul. 31 (2005), pp. 1027–1033.
[47] M.M.T. Dagama and K.E. Gubbins, *Adsorption and orientation of amphiphilic molecules at a liquid–liquid interface*, Mol. Phys. 59 (1986), pp. 227–239.
[48] H. Dominguez and M.L. Berkowitz, *Computer simulations of sodium dodecyl sulfate at liquid/liquid and liquid/vapor interfaces*, J. Phys. Chem. B 104 (2000), pp. 5302–5308.
[49] G.L. Gaines, *Insoluble Monolayers at Liquid–Gas Interfaces*, Wiley, New York, 1966.
[50] F. Ravera, E. Santini, G. Loglio, M. Ferrari, and L. Liggieri, *Effect of nanoparticles on the interfacial properties of liquid/liquid and liquid/air surface layers*, J. Phys. Chem. B 110 (2006), pp. 19543–19551.
[51] F. Reincke, S.G. Hickey, W.K. Kegal, and D. Vanmaekelbergh, *Spontaneous assembly of a monolayer of charged gold nanocrystals at the water/oil interface*, Angew. Chem. Int. Edn. 43 (2004), pp. 458–462.
[52] F.H. Reincke, W.K. Kegel, H. Zhang, M.A. Nolte, D. Wang, D.A.M. Vanmaekelbergh, and H. Möhwald, *Understanding the self-assembly of charged nanoparticles at the water/oil interface*, Phys. Chem. Chem. Phys. 8 (2006), pp. 3828–3835.
[53] M.R. Morrow, D. Singh, D. Lu, and C.W.M. Grant, *Glycosphingolipid acyl chain orientational order in unsaturated phosphatidylcholine bilayers*, Biophys. J. 64 (1993), pp. 654–664.
[54] F.L. Dong, Y. Li, and P. Zhang, *Mesoscopic simulation study on the orientation of surfactants adsorbed at the liquid/liquid interface*, Chem. Phys. Lett. 399 (2004), pp. 215–219.
[55] M.C. Messmer, J.C. Conboy, and G.L. Richmond, *Observation of molecular ordering at the liquid–liquid interface by resonant sum-frequency generation*, J. Am. Chem. Soc. 117 (1995), pp. 8039–8040.
[56] J.C. Conboy, M.C. Messmer, and G.L. Richmond, *Investigation of surfactant conformation and order at the liquid–liquid interface by total internal reflection sum-frequency vibrational spectroscopy*, J. Phys. Chem. 100 (1996), pp. 7617–7622.